Robotica (1997) volume 15, pp 11–22. © 1997 Cambridge University Press

Design of a neurofuzzy algorithm-based shared controller for telerobot systems

D.H. Cha* and H.S. Cho†

SUMMARY

This paper proposes a novel design method of a shared controller for telerobot systems. A shared controller can enlarge a reflected force by combining force reflection and compliance control. However, the maximum boundary of the force reflection gain guaranteeing the stability greatly depends upon characteristics of the elements in the system such as; a master arm which is combined with the human operator's hand, the environments where the slave arm contacts and the compliance controller. In normal practice, it is therefore, very difficult to determine such a maximum boundary of the gain. To overcome this difficulty, the paper proposes a force reflection gain-selecting algorithm based on neural network and fuzzy logic features. The method estimates characteristic of the master arm and the environments by using neural networks, and then, determines the force reflection gain from the estimated characteristics by using fuzzy logic. The algorithm can work in an on-line manner, and can be easily applied to any telerobot system because it requires no a priori knowledge on the system. The effectiveness of the proposed control scheme is verified through a series of experiments using a laboratory-made telerobot system.

KEYWORDS: Neurofuzzy algorithm; Telerobot systems; Force rejection gain; Shared control.

1. INTRODUCTION

A telerobot system is generally composed of a master arm which is controlled by a human operator and a slave arm which duplicates the motion of the master arm and performs actual works in a remote site. In a typical telerobot system with no force reflection or compliance control, a stiff slave arm strictly follows the motion of a master arm. To achieve more complex tasks, however, such a system may be unsuitable because of insufficient information on the working environment. The forces exerted by a slave arm interacting with the environment contain much information on the teleoperation processes or working environments. The use of force information, therefore, can greatly improve the task performance. Two major techniques that utilize the contact forces are compliance control and bilateral control.

In the compliance control system,[1–4] the contact forces are not reflected to the operator but used for the compliance control of a slave arm. An operator assigns reference trajectory to a slave arm through a master arm and the forces are fed back to a compliance controller. The compliance controller, then, generates corrective motions and these are superimposed to the reference trajectory, and as a result, a modified reference trajectory is generated. In a bilateral control system,[5–7] the contact forces are reflected to a human operator via the master arm so that he/she can correct his/her motions according to these forces. Such a system is also called as a force reflection system, and the force reflection can significantly enhance the task performance. The larger the force reflection gain is, the bigger the reflected force becomes. However, the gain should be bounded into a certain value because of the instability problem.[8]

To enlarge the reflected force, many shared control algorithms have been proposed by combining the bilateral control and the compliance control.[8–10] In these schemes, a slave arm becomes more compliant by employing compliance control, and therefore, it is possible to enlarge the reflected force. Thus, good task performance can be assured.

Hannaford[9] studies the effect of compliance loop on stability and performance in the shared control, and showed that the compliance control at the slave side can reduce instability problem. Goldenberg[10] proposed an advanced bilateral control algorithm where the reflected force was derived from the velocity error and contact force. This scheme, however, requires the perfect model of the master arm. Kim[8] found out a stable limit of the force reflection gain using the open-loop transfer function, and proposed the low-pass-filtered bilateral control algorithm which can considerably increase the force reflection gain.

In spite of the previous studies, there still remains an unsolved problem; how to determine a force reflection gain under the uncertain characteristics of master and environments. In the shared control, the force reflection gain greatly affects the task performance of the system: too small gain results poor performance while too large gain makes the system to be unstable. To ensure good performance, the gain should be adequately adjusted by guaranteeing the stability of the system. However, the

* Department of Mechatronics, Samsung Institute of Management and Technology, Nongsori 14-1, Gihung, Yongin, Kyungki-do, (Korea) e-mail: dhcha@samsung.co.kr.
† Department of Mechanical Engineering, Korea Advanced Institute of Science & Technology, Kusongdong 373-1, Yusonggu, Taejon (Korea) e-mail: hscho@lca.kaist.ac.kr, hscho@sorak.kaist.ac.kr.

https://doi.org/10.1017/S0263574797000039 Published online by Cambridge University Press

maximum boundary of the gain greatly depends upon characteristics* of the elements in the system such as; a master arm which is combined with the human operator's hand, a slave arm, a compliance controller, and the environments with which the slave arm contacts. In many cases, the slave arm is required to work in uncertain environments, and thus, the characteristics of the environments can be assumed to be unknown and significantly change according to the task to be done.[3] Also, it has been reported that the characteristics of the master† are changing significantly whether the operator holds the master with a firm or loose grasp.[7,11] Furthermore, the master shows highly nonlinear characteristics which still remains unknown. In normal practice, it is therefore, very difficult to determine the maximum boundary of the force reflection gain.

To overcome this difficulty, the paper proposes a force reflection gain selecting algorithm based on neural network and fuzzy logic features. The method estimates characteristics of the master arm and the environments using neural networks, and then, determines the force reflection gain using fuzzy logic based upon the estimated characteristics. The algorithm can work in an on-line manner, and can be easily applied to any telerobot system because it requires no a priori knowledge. The effectiveness of the presented algorithm is verified through a series of experiments under various conditions of teleoperation using a laboratory-made telerobot system.

The paper is organized as follows: Section 2 describes the telerobot system used in the study. In section 3, the factors affecting task performance and stability are briefly discussed to present a guide line for determining the force reflection gain. Section 4 shows the detailed algorithm of the proposed method, and section 5 discusses the experimental procedure and results. Finally, some conclusions are made in section 6.

2. THE TELEROBOT SYSTEM

Figure 1 shows the telerobot system developed at the Laboratory for Control Systems and Automation (LCA) in the Korea Advanced Institute of Science and Technology. The system consists of a force reflective master arm, a slave arm and a system controller. The master arm has a vertical articulated structure with three degrees of freedom (d.o.f.). Three D.C. servo motors with harmonic drives are mounted in each axis. To reduce friction, each motor is directly connected to the rotational shaft of each axis. To enhance maneuverability, balancing weights are attached to the second and third axes. Three axis-control boards are developed as torque controllers. The slave arm is an industrial robot (Samsung, FARA A1-U) which has a vertical articulated structure with six d.o.f. A joint position control (JPC) board, used as a slave arm controller, controls angular positions of the six joints of the arm.[12]

A six axes force/torque sensor (ATI, FT 30/100) is attached at the end of the slave arm to measure the

* In this paper, the term "characteristics" of a system means "dynamic characteristics" of the system, such as impedance(stiffness) or admittance(compliance).
† From now on, the term "characteristics of master arm" implies "the characteristics of master arm combined with the operator's hand".

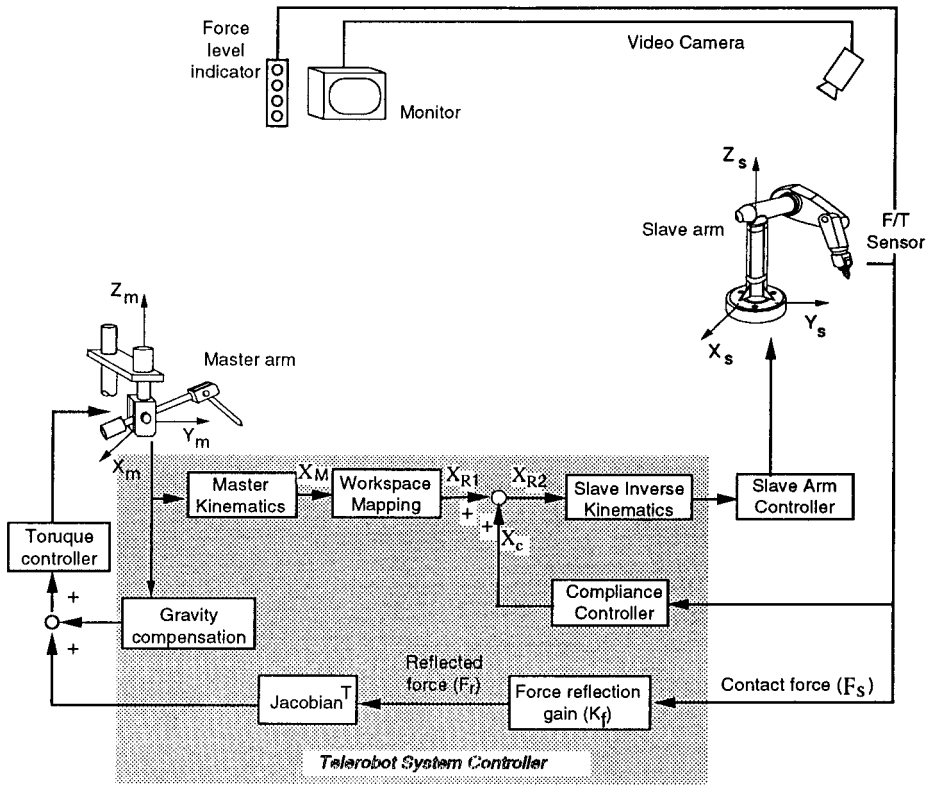

Fig. 1. The structure of the LCA telerobot system.

https://doi.org/10.1017/S0263574797000039 Published online by Cambridge University Press

force/moment. To provide visual information of the contact force, a force level indicator composed of 16 light emitting diodes (LED) with a bar graph arrangement is installed at the operator site. Although the human operator can feel the contact force through the master arm, addition of visual feedback of force can enhance task performance significantly during the experiments. To monitor the slave environment, a CCTV camera is installed at the ceiling of the working site.

The telerobot system controller implemented by a PC 486/DX2-66 is composed of a master arm kinematics routine, a workspace mapping routine, a slave arm inverse kinematics routine, a compliance controller and a force reflection controller. Since the master and slave arms have kinematically different structures, workspace mapping is required so that a position of the master arm, X_M, can be appropriately transformed to the corresponding space of the slave arm, X_S. The detailed algorithm is similar to that described in reference 13. The contact force measured by the force/torque sensor is converted to the froce with respect to the base coordinate of the slave arm. The reflected force is evaluated by multiplying the contact force by the force reflection gain, and then, the resultant is converted to the torque applied at each axis of master arm through the transpose of the master Jacobian. The master and slave controllers are connected with a main PC through the PC-AT bus via two parallel I/O boards.

3. FACTORS AFFECTING TASK PERFORMANCE AND STABILITY

Figure 2 shows a typical block diagram of a shared control of a telerobot system. The controller consists of a compliance controller and a force reflection controller. The compliance controller constitutes an inner feedback loop, while the force reflection controller constitutes an outer feedback loop. When contact force occurs, the compliance controller receives this force as an input and generates corresponding corrective motion, X_C, as an output. This corrective motion is superimposed on the master arm trajectory, X_{R1}, and as a result, a modified reference trajectory, X_{R2}, is generated. At the same time, the contact force is also reflected back to the human operator through the master arm after scaling by a force reflection gain, k_f.

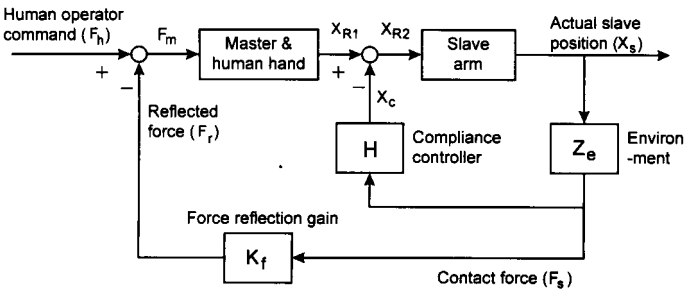

Fig. 2. A typical block diagram of the shared control.

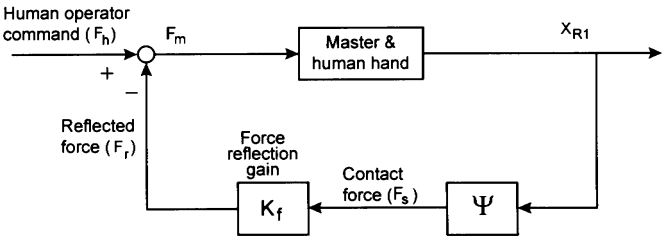

Fig. 3. A simplified block diagram of the shared control.

3.1 Effects of the force reflection gain

Figure 3 shows a simplified block diagram of a shared control system, where Ψ denotes the compliance loop, i.e. a resultant function of the slave, the environment and the compliance controller. In this system, the contact forces measured by the force/torque sensor are reflected back to the human operator through the master arm after scaling by a force reflection gain, k_f. This forms a closed loop system and causes a trade-off between task performance and stability.

To investigate the effect of the force reflection gain, let us consider a stability condition of the system shown in Figure 3 by following a similar procedure described in Cha[7] et al. Generally, the master arm, slave arm and environments can be considered as nonlinear systems. If we use the small gain throrem[14] for stability of such a system, its sufficient condition can be obtained by

$$\begin{aligned} \|[M(F_m)]_T\| &\le \gamma_1 \|(F_m)_T\| \quad \forall T \ge 0, \quad \forall F_m \in L_{2e} \\ \|[k_f \cdot \Psi(X_{R1})]_T\| &\le \gamma_2 \|(X_{R1})_T\| \quad \forall T \ge 0, \quad \forall X_{R1} \in L_{2e} \end{aligned} \tag{1}$$

$$\gamma_1 \cdot \gamma_2 \le 1$$

where $M(\cdot)$ denotes a function for master arm, while $\|\cdot\|$ denotes the function norm and $(\cdot)_T$ denotes the projection operator defined by

$$f_T(t) = \begin{cases} f(t) & \text{if } t \le T \\ 0 & \text{if } t > T. \end{cases} \tag{2}$$

The above equations mean that the system is BIBO (bounded input bounded output) stable if the loop gain is less than unity.[15] To show the effect of the force reflect gain more clearly, let the DC gains of M and Ψ be denoted by M_0 and Ψ_0, respectively. Then, the DC loop gain, G_{DC} should be less than unity for the system to be stable,[8] i.e.

$$G_{DC} = k_f \cdot \Psi_0 \cdot M_0 \le 1 \tag{3}$$

Namely,

$$k_f \le \frac{1}{Z_{e0} \cdot \Psi_0} \tag{4}$$

Note that Ψ_0 contains the slave, the environments and the compliance controller. From these equations, then, it can be seen that the force reflection gain should be determined under the consideration of characteristics of the master, the slave, the environments and the compliance controller.

A small force reflection gain results in a small reflected force, and thus, the operator hardly feels the contact

https://doi.org/10.1017/S0263574797000039 Published online by Cambridge University Press

force so that task performance becomes poor. On the other hand, a large gain results in a large reflection force, thus, ensuring good task performance, however, too large gain causes instability. From these facts, it can be seen that there is a trade-off between stability and task performance.

3.2 *Effects of the compliance loop*

Effect of the compliance controller can be seen to decrease the effective stiffness of a slave arm.[8] The higher the gain of the compliance controller is, the lower the effect stiffness of the slave arm becomes. However, the gain of the compliance controller should be limited because too large gain makes the system unstable. To concisely investigate the stable condition of the compliance loop shown in Figure 2, let us following a similar procedure described in the above section. Let S denotes the slave arm, and DC gains of S, H and Z_e be denoted by S_0, H_0 and Z_{e0}, respectively. The DC loop gain, G_{DC}, then, should be less than unity for the system to be stable, i.e.,

$$G_{DC} = H_0 \cdot Z_{e0} \cdot S_0 \leq 1 \tag{5}$$

Namely,

$$H_0 \leq \frac{1}{Z_{e0} \cdot S_0} \tag{6}$$

From these equations, it can be seen that a compliance controller should be determined under the consideration of characteristics of the slave arm and the environments.

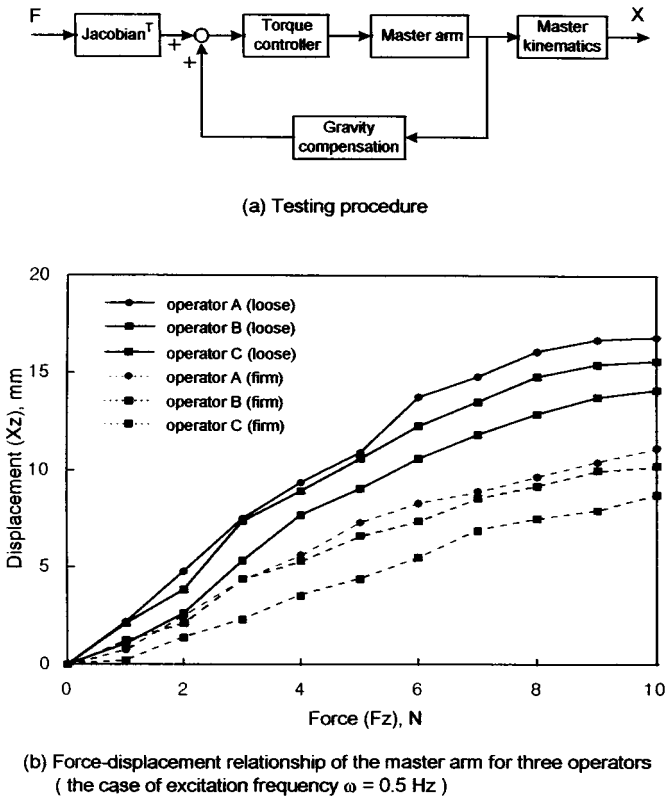

Fig. 4. Compliance characteristics of the LCA master arm (a) Testing procedure (b) Force-displacement relationship of the master arm for three operators (the case of excitation frequency $\omega = 0.5$ Hz).

3.3 *Characteristics of master, slave arm and environments*

The compliance characteristics of the master arm changes significantly depending upon how the operator holds the master arm.[6,7] To investigate the characteristics of the master arm shown in Figure 1, some experiments were performed as shown in Figure 4(a). The z-directional force, $F = F_Z \sin \omega t$, was given as the reference value for the torque controller and the corresponding motion of the master arm, $X = X_Z \sin(\omega t + \phi)$, was measured. During the experiment, the motion of the master arm was not transferred to the slave, and thus, the slave did not move. The experiments were conducted by three operators, and the excitation frequency, ω, was set to the two values, 0.5 Hz and 2 Hz, which were the minimum and the maximum frequency values used in Uebel's study.[16] From the results shown in Figure 4(b), it can be seen that the compliance characteristics of the master significantly change according to the operator's working mode and show nonlinear relationships. Also, they change significantly with respect to the operator. Although the results has not been shown here due to space limitation, the effect of frequency was found to be small compared with those of operator's mode, which is similar to those in reference 7.

In many cases, the slave arm is required to operate in uncertain or even unknown environments, and thus, characteristics of the environment are often assumed to be unknown with nonlinearities.[3] Also they change significantly depending upon the type of the task to be done.

In some telerobot systems, industrial manipulators are frequently used as slave arms. As typical industrial manipulators are controlled by position serve systems with high servo gains and high gear ratio, their dynamics can be represented by a second order linear system with constant parameters.[17,18] In this study, therefore it is assumed that the dynamic characteristics of the slave arm remains unchanged.

4. THE NEUROFUZZY ALGORITHM-BASED SHARED CONTROLLER

Figure 5 shows the block diagram of the proposed algorithm. The shared controller consists of a first-order linear compliance controller, a force reflection gain, and a force reflection gain selecting algorithm. First, the force reflection gain selecting algorithm is presented, and then, a design criteria of the compliance controller is described.

4.1 *The force reflection controller*

The force reflection controller consists of a force reflection gain selecting algorithm and a force reflection gain. The force reflection gain selecting mechanism, which is similar to that of the previous work,[7] consists of two multi-layered neural networks, a fuzzy gain selector and a decision maker. The characteristics of the master

https://doi.org/10.1017/S0263574797000039 Published online by Cambridge University Press

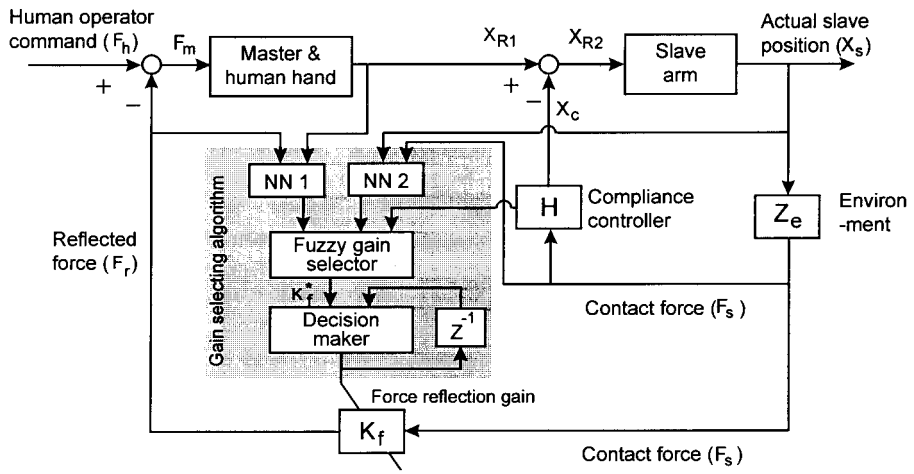

Fig. 5. The block diagram of the proposed algorithm.

arm and environments are classified by the NN1 and NN2, respectively. The fuzzy gain selector determines the inferred force reflection gain, k_f^*, based upon the estimated characteristics and the compliance characteristic of the compliance controller. Finally, a decision maker determines whether or not the present gain, k_f, should be updated with the new one inferred from the fuzzy gain selector.

4.1.1 **Neural classifier.** Now, the problem at hand is to classify characteristics of the master and the environments which have nonlinearity and undergo significant change depending upon working conditions. Unfortunately, it is very difficult to classify the characteristics of the master arm in an on-line manner and little classifying method has been reported. One solution to this problem is to utilize artificial neural network. The neural classifier used herein consists of two multi-layered neural networks, NN 1 and NN 2. Their objectives are to classify the dynamic characteristics of the master and environments in an on-line manner. The NN 1 received the reflected-force data and position information of the master arm as inputs, and produces an output, m, which is a value between zero and unity representing the characteristics of the master arm. On the other hand, the NN 2 received the position and force information of the slave arm as inputs, and yields an output, z, ranging between a value between zero and unity, which represented characteristics of the environment.

Table I Various conditions of the operator and the environments

No.	Operator's working mode	Environment
1	firm	styrofoam
2	loose	styrofoam
3	firm	rubber
4	loose	rubber
5	firm	steel
6	loose	steel
7	firm	plastic
8	loose	plastic
9	firm	silicon
10	loose	silicon

(a) **Actual network training.** Now, the experiments performed to train the neural classifier will be discussed. Three operators conducted a series of experiments under ten different conditions of the master arm and environments as shown in Table I. During the experiments, direction of the end effector of the slave arm is fixed at a constant direction ($-Z_S$ direction) with respect to the global reference coordinates. The task performance in the experiments was to maintain a constant contact force of 20N in z-direction as shown in Figure 6(a). During the experiments, the force reflection gain was set to 0.1, and the compliance controller,

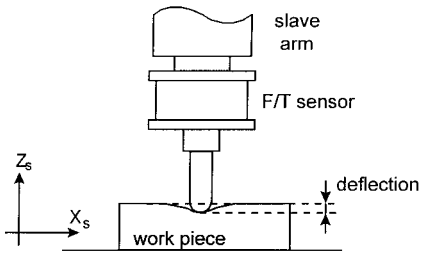

(a) Testing procedure

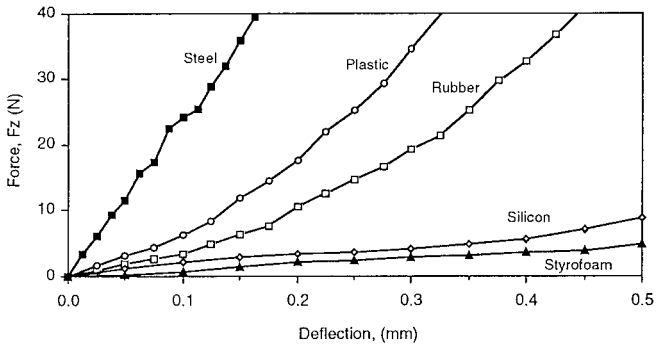

(b) Effective stiffness of various workspieces

Fig. 6. Effective stiffness of various workpieces (a) Testing procedure (b) Effective stiffness of various workpieces.

https://doi.org/10.1017/S0263574797000039 Published online by Cambridge University Press

$H(s) = h/(\tau s + 1)$, was set to $h \times 4 \times 10^{-6}$ and $\tau = 0.1$. All data were collected at 62.5 Hz. Figure 6(b) shows the effective stiffness of the various workpieces used in the experiments. Here, the *effective stiffness* means a combined stiffness of the workpiece and the end effector of slave arm.

Although three directional positions and forces (x, y and z-direction) were measured, only z-directional data were used for the training. Generally, all positions and forces can be collected during the teleoperation, but if it is assumed that the characteristics of master and environment have isotropic properties, only one directional position and force data are sufficient to classify their characteristics. The above assumption can be adopted in most of teleoperation.

The main feature of training the multi-layered neural network is to learn the relationship between the inputs and outputs. Thus, determination of suitable data for inputs and outputs are one of the essential issues in practical implementation of the neural classifier. To obtaining the suitable data set, training the neural networks was conducted under various sets of inputs and outputs as shown in Table II.

Among ten data sets collected, the six data set (No. 1–6 in Table I) were presented to the networks for training. First, six data composed of three position data of the master arm and three reflection force data, were given as the inputs for NN 1. In a similar way, six data, three position data of the slave arm and three contact force data, were given as inputs for NN 2. The inputs are given in Table II in detail. The target outputs for the NN 1 and NN 2 were assigned as values between zero and unity, and are given in Table II. Both the two networks have 60-20-10-1 nodes. Training was conducted using the error back propagation algorithm[19] until the number of iteration reaches 20,000. The total number of the training sample was 2,400.

Table II Inputs and outputs for the neural classifier

input data for NN		Number of inputs		
NN 1	NN 2	6	8	10
$X_m(t) - X_{mc}$	$X_S(t) - X_{SC}$	O	O	O
$\Delta X_m(t)$	$\Delta X_S(t)$	O	O	O
$\Delta X_m(t-1)$	$\Delta X_S(t-1)$	O	O	O
$\Delta X_m(t-2)$	$\Delta X_S(t-2)$	X	O	O
$\Delta X_m(t-3)$	$\Delta X_S(t-3)$	X	X	O
$F_r(t)$	$F_S(t)$	O	O	O
$\Delta F_r(t)$	$\Delta F_S(t)$	O	O	O
$\Delta F_r(t-1)$	$\Delta F_S(t-1)$	O	O	O
$\Delta F_r(t-2)$	$\Delta F_S(t-2)$	X	O	O
$\Delta F_r(t-3)$	$\Delta F_S(t-3)$	X	X	O

O: included, X: not included.
X_{mc}: the position of the master arm when contact occurs.
X_{SC}: the position of the slave arm when contact occurs.

$$\Delta X_i(t) = X_i(t) - X_i(t-1) \quad (i = m, s)$$
$$\Delta F_i(t) = F_i(t) - F_i(t-1) \quad (i = r, s)$$

Target outputs for NN 1			Target outputs for NN 2	
firm	operator A	1.0		
	operator B	0.82		
	operator C	0.62	styrofoam	0.0
loose	operator A	0.33	rubber	0.5
	operator B	0.23	steel	1.0
	operator C	0.0		

(b) **Results and discussions.** The training results for NN 1 are shown in Figure 7(a). In the figure, the average system error is a mean-square error between the target output and trained output, which is defined by

$$E = \frac{1}{2P} \sum_p (t_p - o_p)^2 \tag{7}$$

where t_p denotes the target output and o_p denotes the output generated by the neural network while the subscript p denotes p-th training sample, and P is the total number of training samples.

From the figure, it can be seen that in the case of six input, the error decreases rapidly in early stage, and thereafter, does not decrease further. The training results for NN 2 given in Figure 7(b) show a similar trend, and the error is not exactly converged to zero. In this case, additional training was performed up to 40,000 iterations,

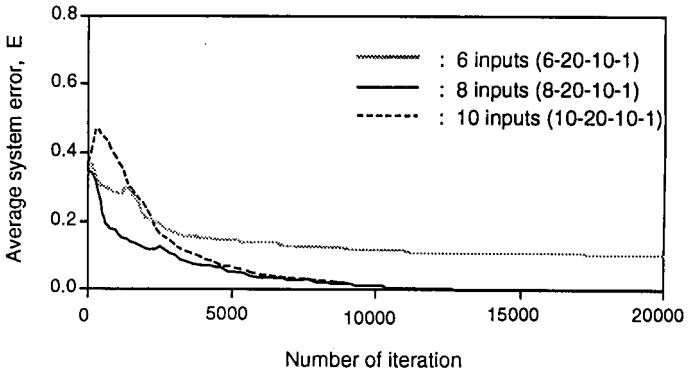

(a) Average system errors for NN1

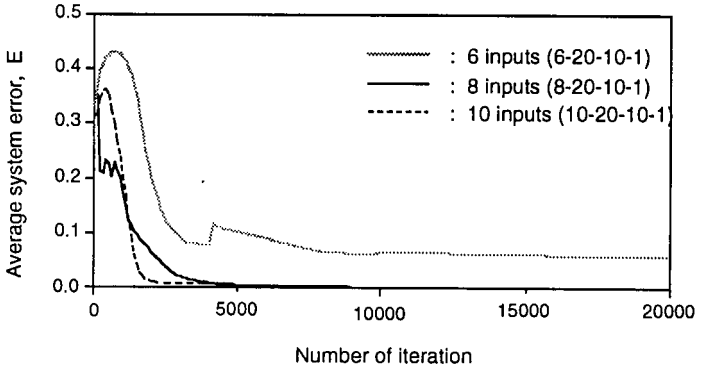

(b) Average system errors for NN 2

Fig. 7. Training results for various number of inputs (a) Average system errors for NN 1 (b) Average system errors for NN 2.

https://doi.org/10.1017/S0263574797000039 Published online by Cambridge University Press

and the result also showed no further decrease in error. If eight and ten data are given as inputs to both the NN 1 and NN 2 as shown in Table II, the results are quite different from those of the previous case: the error converges to zero as shown in the same figure. These results indicate that the train was performed well.

From the above results, it can be seen that, in the case of the six inputs, the NNs can not learn well the characteristics of the master and environments due to the insufficient input data. In the cases of the eight and ten inputs, however, the networks can learn the characteristics of the master and environments. The reason for the results can be explained as follows: In order for a multi-layered neural network to represent the behavior of a dynamic system at time *t,* the previous knowledge of the system (i.e., inputs and outputs of the system before time *t*) should be given to the network as inputs. If the previous knowledge is insufficient, the network can not represent the behaviour of the system.

(c) **Effects of the node size.** One of the main design parameters of the neural network is the number of hidden layers, and the number of nodes in each layer. As these parameters increase, a network can perform more complex mapping. However, the resulting complexity of connections in the network requires more computation time. In this study, two hidden layers were used because they are enough to realize the usual mapping functions.

To investigate the effect of node size, training was conducted for various sizes of the node number in the case of the eight inputs. Figures 8(a)–(b) show the results. In both cases, convergence speed of the 8-15-8-1 networks are found to be very slow, and the final error is much larger than those of other cases. In the cases of 8-20-10-1 and 8-25-15-1, convergence speed appears to be satisfactory.

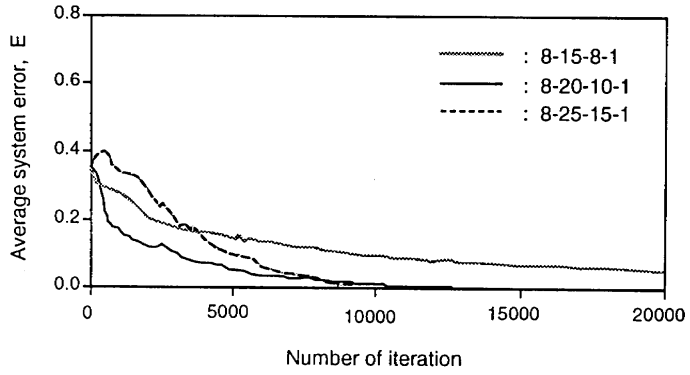

(a) Average system errors for NN1

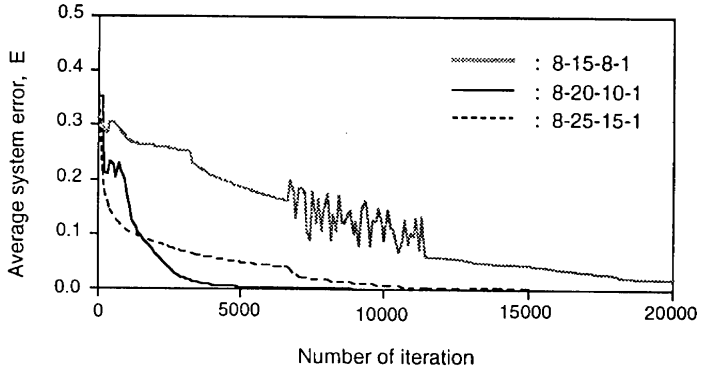

(b) Average system errors for NN 2

Fig. 8. Training results for various number of nodes (a) Average system errors for NN 1 (b) Average system errors for NN 2.

4.1.2 **Fuzzy gain selector.** It is very difficult and yet remains unknown to find out the optimal force reflection gain, even though the characteristics of the master and the environments are known. In most force reflection systems, human operator usually determines the gain based upon his/her experiences and/or knowledge about the teleoperation. Many research works have shown that a fuzzy logic witjh approximate reasoning can emulate the decision-making ability of a skilled human operator.[20] Based upon this reasoning, fuzzy logic can be effectively applied to determine the force reflection gain.

As shown in Figure 5, the inputs of the fuzzy gain selector are two outputs of the neural classifier and a DC gain of the compliance controller, while its output is a force reflection gain. The selector consists of four modules just as the general fuzzy logic controller does: a fuzzy decoder, a rule base, a fuzzy reasoning and a defuzzifier.

(a) **Fuzzy decoder.** The input fuzzy variables are obtained by scaling from the inputs of the fuzzy gain selector and they are defined by

$$\begin{aligned} \tilde{m} &= g_m \times m \\ \tilde{z} &= g_z \times z \\ \tilde{h} &= g_h \times h \end{aligned} \tag{8}$$

where m, z and h denote the output of NN 1, NN 2, and the DC gain of compliance controller, while g_m, g_z and g_h denote scaling factors for m, z and h, respectively.

(b) **Rule base.** In constructing the rule base, there are generally three ways as described in the followings: (1) expert's knowledge or experiences; (2) self-improvement; (3) fuzzy modeling. In this study, the rule base is constructed using the first method. The output variables of the fuzzy rule takes the form of fuzzy singleton, which decreases the calculation time considerably, and thus, profitable in real time application. The rule base consists of 18 rules and takes the form:

$$\text{Rule } R_I\text{: IF } \tilde{m} \textit{ is } M_i, \tilde{z} \textit{ is } Z_i, \tilde{h} \textit{ is } H_i \text{ THEN } \tilde{k}_f^* \textit{ is } K_i \quad (i = 1, 2, \ldots, 18) \tag{9}$$

where the subscript i denotes the i-th rule. Also, M_i, Z_i, H_i and K_i are the fuzzy subsets corresponding to the variables $\tilde{m}$, $\tilde{z}$, $\tilde{h}$ and $\tilde{k}_f^*$, respectively. The fuzzy subsets for each variables are defined as shown in Figure 9 while the 18 rules are shown in Table III.

https://doi.org/10.1017/S0263574797000039 Published online by Cambridge University Press

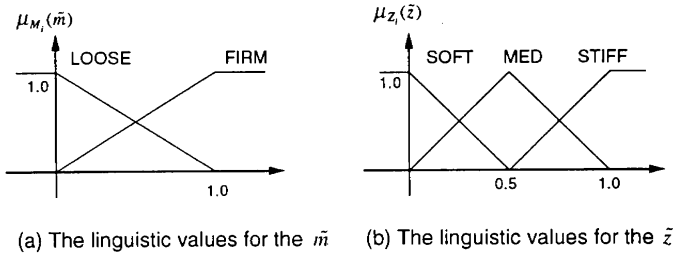

(a) The linguistic values for the $\tilde{m}$ (b) The linguistic values for the $\tilde{z}$

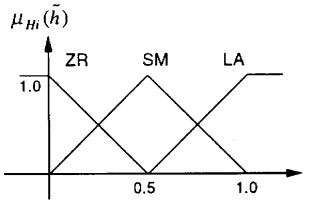

(c) The linguistic values for the $\tilde{h}$

Fig. 9. Definition of the fuzzy linguistic variables (a) the linguistic values for the $\tilde{m}$ (b) The linguistic values for the $\tilde{z}$ (c) The linguistic values for the $\tilde{h}$.

(c) **Fuzzy inference.** For each rule base, the min–max operation is adopted to perform fuzzy inference. Let $\mu_{K_i}(\tilde{k}_i^*)$ be the membership function for a subset of the output which is result of the k-th rule. Then, it can be obtained by

$$\mu_{K_i}(\tilde{k}_i^*) = [\mu_{M_i}(\tilde{m}) \wedge \mu_{Z_i}(\tilde{z}) \wedge \mu_{H_i}(\tilde{h}) \wedge \mu_{K_i}(\tilde{k}_f^*)] \quad (10)$$

where the operator, $\wedge$, denotes the min operation. From the results of the 18 rules, the final membership function, $\mu_K(\tilde{k}_f^*)$, can be obtained by using max operator:

$$\mu_K(\tilde{k}_f^*) = [\mu_{K_1}(\tilde{k}_1^*) \vee \mu_{K_2}(\tilde{k}_2^*) \vee \cdots \vee \mu_{K_{18}}(\tilde{k}_{18}^*)] \quad (11)$$

where the operator, $\vee$, denotes the max operation.

Table III Fuzzy rules for the fuzzy gain selector

(a) in the case of h = ZR

m \ z	SOFT	MED	STIFF
LOOSE	0.3	0.18	0.1
FIRM	0.6	0.25	0.15

(b) in the case of h = SM

m \ z	SOFT	MED	STIFF
LOOSE	0.45	0.25	0.15
FIRM	0.75	0.4	0.2

(c) in the case of h = LA

m \ z	SOFT	MED	STIFF
LOOSE	0.65	0.3	0.2
FIRM	1.0	0.55	0.26

(d) **Defuzzifier.** The proposed algorithm requires a crisp force reflection gain. Thus, a defuzzifier is adopted to yield a crisp gain from the inferred fuzzy gain given in equation (10). The crisp force reflection gain, k_f^*, can be obtained by

$$k_f^* = g_k \times \text{Defuzzify}\{\mu_K(\tilde{k}_f^*)\} \quad (12)$$

where g_k are the scaling factors for $\tilde{k}_f^*$ and Defuzzify $\{\cdot\}$ denotes the defuzzifier operator which performs defuzzification by using the center of gravity method.

4.1.3 **Decision maker.** The ultimate aim of selecting force reflection gain is to enhance the task performance. For such a purpose, the gain selecting algorithm should be designed to have the following properties; if the characteristics of a master or environments are changed, the gain should be changed adaptively. Otherwise, the gain should remain unchanged because gain change causes the operator to be confused, resulting in poor performance.

It can be seen in the experimental results which will be described in the next section in more detail, that the outputs of the neural classifier change slightly even though the characteristics of master or environments remains unchanged (for example, see the results in the Figure 11(a) and (b)). This is due to the imperfect learning capability of the neural networks or inevitable measuring noise contained in the inputs. Such a slight change of the estimated values can be frequently seen in many other classification algorithms working in an on-line manner. In this case, the output of the fuzzy gain selector tends to change slightly. Upon consideration of this fact, it is necessary to design a decision maker which determines whether or not the present gain should be updated with the new one, inferred from the fuzzy gain selector.

Let $k_f(t)$ be the force reflection gain used at time t, and $k_f^*(t)$ be the inferred gain at that time. Then, the decision Π can be defined by

$$\Pi = \alpha_D \cdot \left|1 - \frac{k_f(t)}{k_f^*(t)}\right| + \beta_D \cdot \left|\sum_{i=t_s}^{t} \frac{k_f^*(i) - k_f(i)}{k_f(i)}\right| - C \quad (13)$$

where α_D, β_D $(0 < \alpha_D, \beta_D \leq 1, \alpha_D + \beta_D = 1)$ are the weighting factors and C is a constant, while t_s denotes the time at which the latest gain change had occurred. The first term of the above equation represents the ratio of the present gain to the inferred gain, while the second term represents the accumulated normalize error between the inferred gain and the actual gain since the time t_s. Now, the force reflection gain at time $t+1$ is determined by

$$k_f(t+1) = \begin{cases} k_f^*(t) & \text{if } \Pi \geq 0 \\ k_f(t) & \text{if } \Pi < 0. \end{cases} \quad (14)$$

This indicates that, if Π is greater than zero, the gain is updated, otherwise, it remains unchanged. In other words, the gain is updated when the ratio of the presnt gain to the inferred gain is larger and/or the accumulated normalized error is large.

https://doi.org/10.1017/S0263574797000039 Published online by Cambridge University Press

4.2 The compliance controller

The first order linear compliance controller has a form given by

$$H(s) = \frac{h}{\tau s + 1} \tag{15}$$

where h and τ denote the DC gain and the time constant of the controller, respectively. Applying equation (6), h should be bounded

$$h \leq \frac{1}{Z_{e0} \cdot S_0} \tag{16}$$

Larger value of the time constant, τ, can enlarge stable region of telerobot system.[21] On the other hands, from many studies to establish required bandwidth of telerobot systems,[16,22,23] it can be concluded that the bandwidth of a telerobot system should be greater than 5 Hz. Therefore, the time constant should be limited within a certain boundary so as to satisfy the bandwidth requirements of telerobot systems.

5. EXPERIMENTS AND RESULTS

In this section, two types of experiments were conducted: first, the experiments with fixed force reflection gains were conducted to investigate the effect of the force reflection gain on the task performance. Second, the experiments with the proposed algorithm were conducted to show the effectiveness of the proposed algorithm, and the results were compared with those of the first ones.

A DC gain, h, of the compliance controller can be determined using equation (16). To determine h, it should be known that the DC gain of environments, Z_{e0}, and slave arm, S_0. The Z_{e0} can be found in the effective stiffness of various environments shown in Figure 6(b). In the figure, the effective stiffness of steel is largest and its value is 2.35×10^5 N/m. Since the slave arm can be represented by a second order linear system with unit DC gain, the S_0 can be treated as an unity. Now, if equation (16) is applied, h should be bounded by

$$h < \frac{1}{2.35 \times 10^5 \times 1} = 4.26 \times 10^{-6}$$

Thus, the h is designed to be 4.0×10^{-6}. Since the bandwidth of a telerobot system should be greater than 5 Hz, the time constant, τ, is designed to be 0.1, which has a bandwidth of 10 Hz.

5.1 Shared control with fixed force reflection gains

The task was the same as that described in the previous section, which was to maintain a constant contact force (20 N) in z-direction. Experiments were conducted under various values of the force reflection gain. In the following experiments, traditional shared controller shown in Figure 2 was used. The operator B in Figure 4 conducted the task in the case of FIRM-Silicon (Case 9 in Table I), and some of the results are shown in Figure 10.

When the gain is 0.1, the human operator can hardly feel the reflection force during the task, and therefore, the results were far from satisfaction. When the gain was 0.2, the results were better than those of the previous, but these were still unsatisfactory. When the gain was 0.4, the results were fairly good because the contact

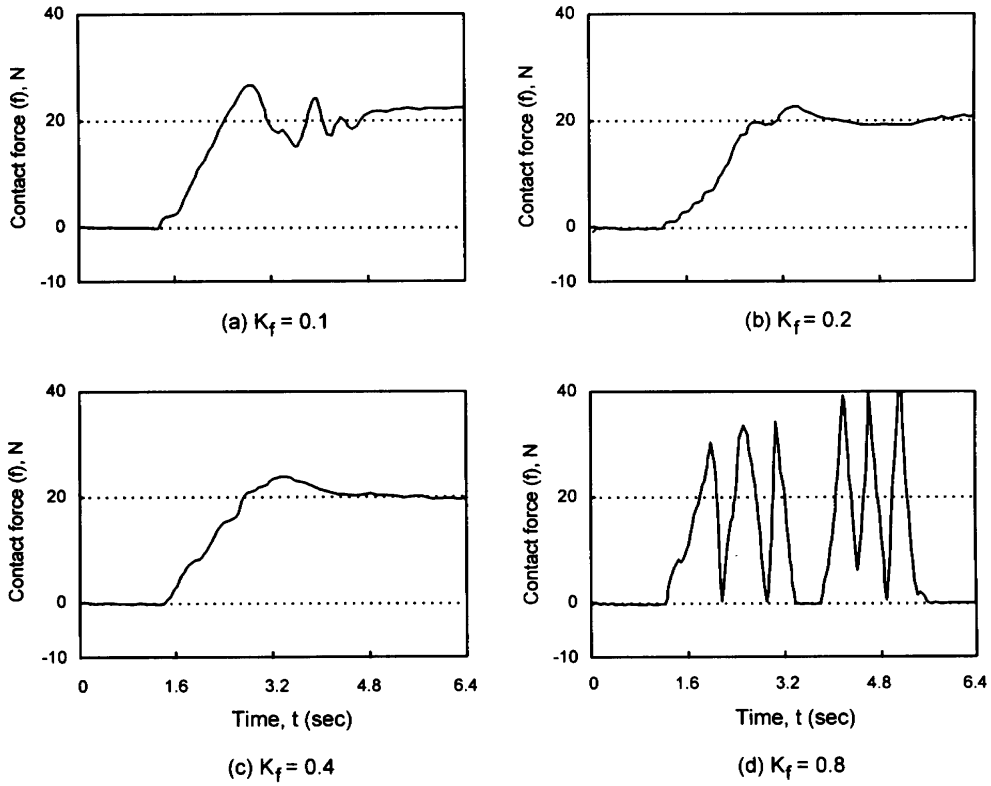

Fig. 10. Results of the contacting experiments with various fixed force reflection gains (the case of FIRM-Silicon).

https://doi.org/10.1017/S0263574797000039 Published online by Cambridge University Press

forces were maintained near the desired value. However, when the gain was 0.8, unstable contact occurred.

From the above results, it can be seen that too small gain results in poor task performance while too large gain results in system instability. This implies that force reflection gain is critical to task performance.

5.2 Shared control with the force reflection gain selecting algorithm

To show the effectiveness of the proposed algorithm, a series of experiments was conducted with the proposed controller in an on-line manner under two different conditions of the master and environments as shown in Table I (Case 7–10). Two types of tasks were conducted; (1) to maintain a constant contact force of 20 N in z-direction, and (2) a peg-in-hole task. When contact occurs, the neural classifier identifies the characteristic of the master and the environments. Then, the fuzzy gain selector and the decision maker determine the new reflection gain based on the identified characteristics. As a result, the operator can conduct the task with this new gain.

In the following experiments, the initial force reflection gain was assigned 0.1. Both the NN 1 and the NN 2 have 8-20-10-1 nodes, and the four scaling factors of the fuzzy selector, g_m, g_z, g_h and g_k were assigned to 0.1, 0.1, 1×10^5, and 0.1, respectively. The two weighting factors of the decision maker, α and β, were set to 0.9 and 0.1, respectively, while the threshold, C, was set to 0.24.

(i) **Contacting task.** First, the experiments were conducted in the case of FIRM-Silicon with the operator B. Figure 11(a) show the results. In the figures, it can be seen that contact occurred at about 1.8 sec. The outputs of the NN 1 and the NN 2 were all zero before the contact, while these became close to 0.82 and 0.2 after the contact, respectively. Note that the target value for NN 1 was 0.82 at the FIRM mode for the operator B, and the target values for NN 2 were 0.0 and 0.5 at styrofoam and rubber, respectively, during the training of neural classifier. Considering these facts, the results indicate that the human operator was working on FIRM mode, and the environment was stiffer than styrofoam

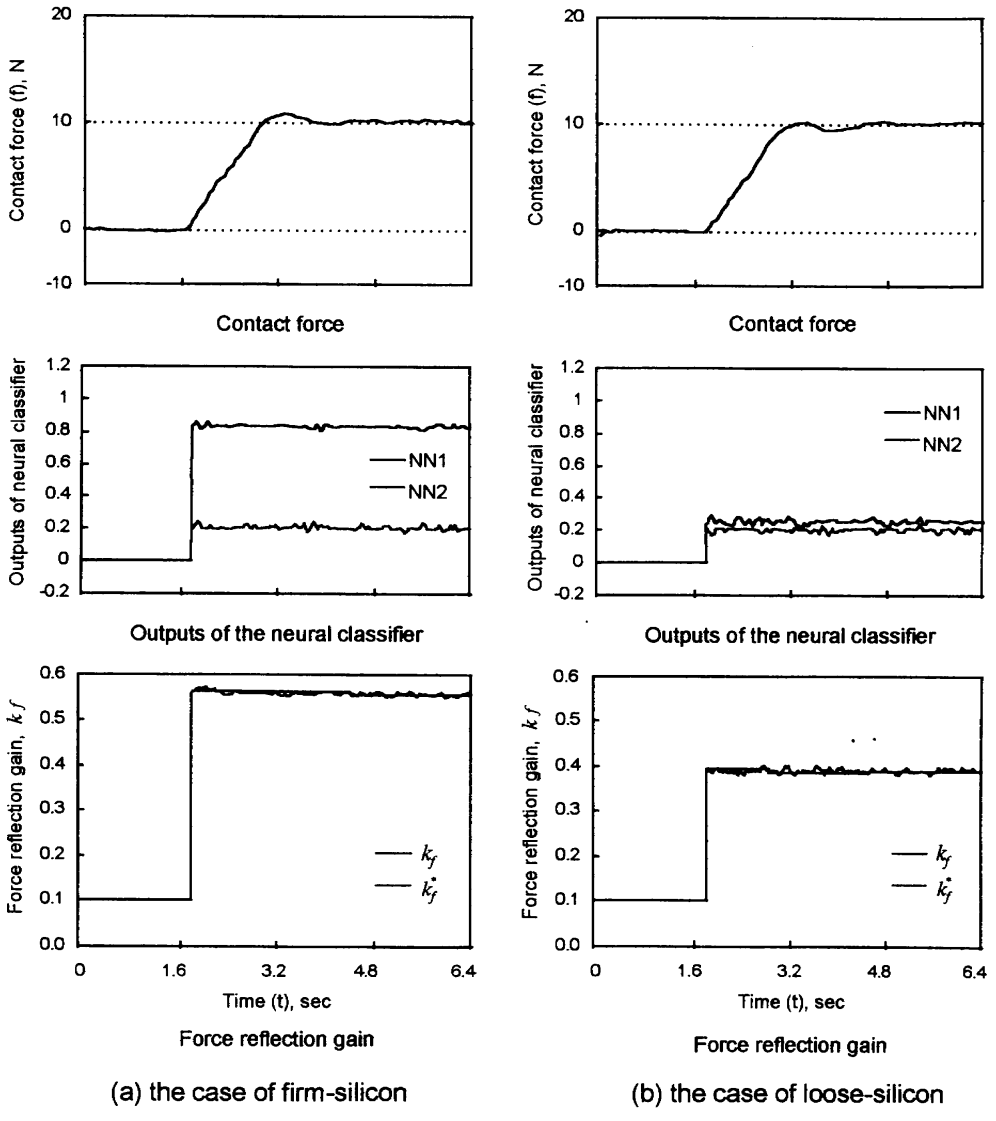

Fig. 11. Results of the contacting experiments for silicon.

https://doi.org/10.1017/S0263574797000039 Published online by Cambridge University Press

but softer than rubber. Also, it can be seen that the outputs of the NN 1 and NN 2 vary slightly after the contact. It should be noted from the results that, although the data obtained in this case had never been used in the training process, the neural classifier could successfully identify characteristics of the master and the environments.

Bottom figure of Figure 11(a) shows the output of the fuzzy gain selector, k_f^*, and the force reflection gain, k_f, which is the output of the decision maker. The k_f^* had its initial value, 0.1, before the contact, while it became close to 0.56 after the contact. As the outputs of NN 1 and NN 2 varied slightly, the k_f^* accordingly varied slightly. The k_f, however, was kepe a constant value, and thus, it can be seen the decision maker behaved well. The contact forces after 4.0 sec were very close to the desired value, 20 N. Note that as the contact force was controlled by the human operator, the results did not show the exact value of 20 N.

Figures 11(b) show the results in the case of LOOSE-Silicon. It can be seen that the neural classifier also worked well in this case. The output of the NN 1 denotes that the operator was working on the LOOSE mode and that the output of the NN 2 shows values similar to those in the case of FIRM-Silicon. From the results, we can also see that the reflection gain, k_f, was updated during the operation by the decision maker according to the equations (13)–(14).

(ii) **Peg-in-hole task.** Now, a peg-in-hole task was done as an another example. A peg was made of polyethylene and its diameter was 20 mm while a hole made of steel has its diameter of 20.4 mm with chamfer of 45 degrees. In the following experiments, the proposed algorithm is only implemented to the translation in x, y and z-axes for the simplicity. During the experiments, direction of the end effector of the slave arm is fixed to a constant direction ($-Z_S$ direction) with respect to the global reference coordinates, and all the other conditions were the same as those of the previous experiments.

The operator C in the Figure 4 conducted the task with the firm and loose modes. The results are shown in Figure 12(a). As can be seen in the figure, the contact occurred at about 3.0 sec, and the outputs of the NN 1 and the NN 2 were also zero before the contact. These became close to 0.57 and 0.62 after the contact,

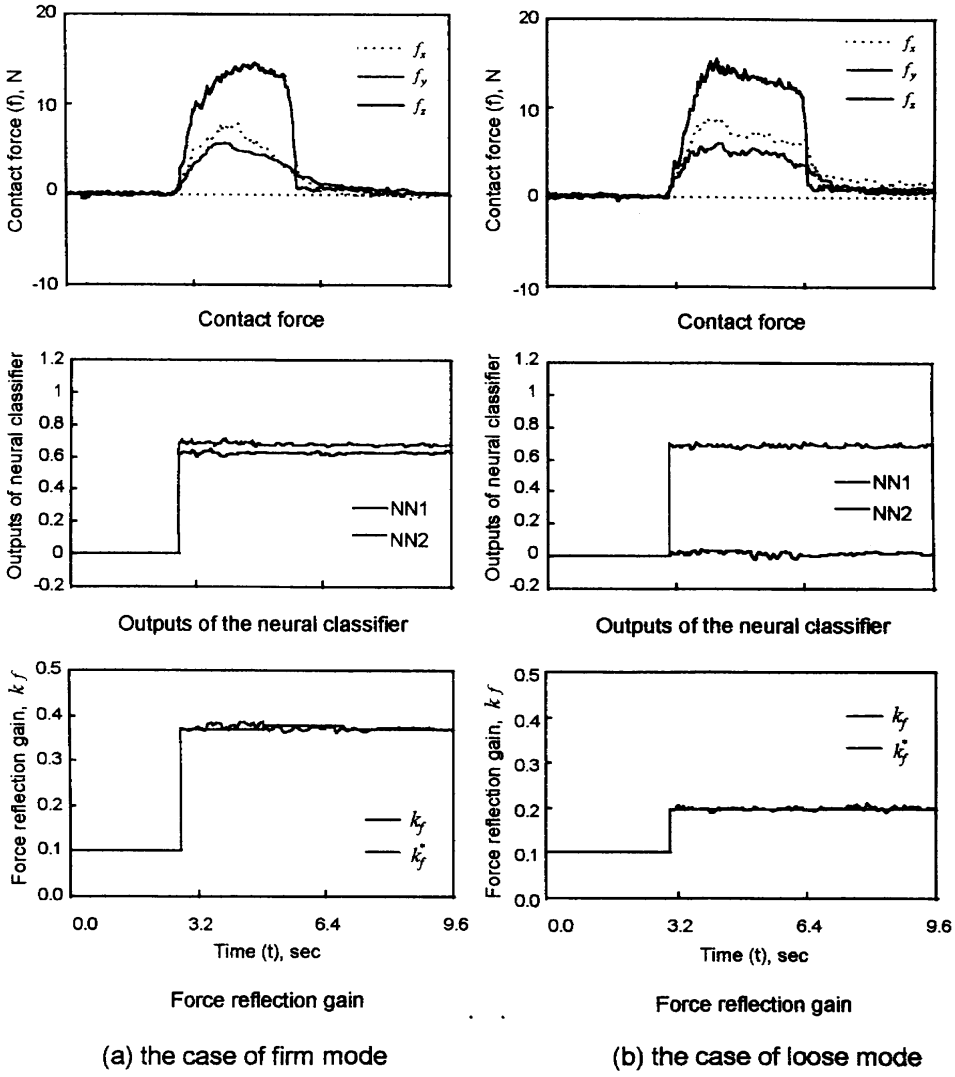

Fig. 12. Results of the peg-in-hole experiments.

https://doi.org/10.1017/S0263574797000039 Published online by Cambridge University Press

respectively. The above results indicate that the operator C was working on firm mode, and the environments was stiffer than rubber but softer than steel. Also, it can be seen that the outputs of NN 1 and NN 2 vary slightly after the contact. It should be noted that, although the data obtained in this task had never been used in the training process, the neural classifier can successfully identify characteristics of the master and the environments. Before the contact, the k_f* had its initial value, 0.1, while it became close to 0.37 after the contact. Figure 12(b) shows similar results. From the figures, it can be observed that the proposed algorithm also behaved well, adopting to changing environment.

6. CONCLUSIONS

A novel design method of a shared controller using neurofuzzy algorithm has been proposed. A shared controller can enlarge the reflected force by combining force reflection and compliance control. In a shared controller, determination of the force reflection gain guaranteeing stability largely depends upon characteristics of a master arm and environments which are uncertain or even unknown. The proposed algorithm estimates characteristics of the master arm and environments using two multi-layered neural networks, and then, determines the force reflection gain based upon the estimated characteristics using fuzzy logic.

From the experimental results using a laboratory-made telerobot system, it can be seen that the characteristics of the master arm combined with the operator and environments significantly change with respect to the working conditions. Also, the well-trained neural classifier can identify these characteristics, and the fuzzy gain selector can effectively determine a force reflection gain which ensures good task performance even under the changing environment and dynamic characteristics of a master arm. Moreover, the algorithm can work in an on-line manner, and can be implemented to any shared telerobot system.

References

1. W.S. Kim, ''Shared compliant control: A stability analysis and experiments'' *Proc. IEEE Int. Conf. Robotics and Automation* (1990) pp. 620–623.
2. K. Kosuge, A. Sato and K. Juruta, ''Task-oriented control of master-slave manipulators'' *Proc. Japan–U.S.A. Sym. on Flexible Automation* (1990) pp. 387–393.
3. S.T. Venkataraman, S. Gulati et al., ''A neural network based identification of environments models for compliant control of space robots' *IEEE Trans. Robotics and Automation* **9,** No. 5, 685–697 (1993).
4. D.H. Cha, and H.S. Cho, ''A neurofuzzy model-based compliance controller with application to a telerobot system'' *Control Engineering Practice* **4,** No. 3, 319–330 (1996).
5. B. Hannaford and R. Anderson, ''Experimental and simulation studies of hard contact in force reflecting teleoperation'' *IEEE Int. Conf. Robotics and Automation* (1988) pp. 584–589.
6. G.J. Raju, G.C. Verghese and T.B. Sheridan, ''Design issues in 2-port network models of bilateral remote manipulation'' *Proc. IEEE Int. Conf. Robotics and Automation* (1989) pp. 1316–1321.
7. D.H. Cha, H.S. Cho an S.K. Kim, ''Design of a force reflection controller for telerobot systems using neural network and fuzzy logic'' *J. Intelligent and Robotic Systems,* No. 1, 1–24 (1996).
8. W.S. Kim, ''Developments of new force reflecting control schemes and an application to a teleoperator training simulator'' *Proc. IEEE Int. Conf. Robotics and Automation* (1992) pp. 1412–1419.
9. B. Hannaford, ''Stability and performance tradeoffs in bilateral telemanipulation'' *IEEE Int. Conf. Robotics and Automation* (1989) pp. 1764–1767.
10. A.A. Goldenberg and D. Bastas, ''On the bilateral control of force reflecting teleoperation'' *Proc. 11th IFAC World Congress* (1990) pp. 215–220.
11. G.J. Raju and T.B. Sheridan, ''An experiment in bilateral manipulation with adjustable impedances'' *Proc. Japan–U.S.A. Symp. on Flexible Automation* (1990) pp. 395–399.
12. S.K. Kim, C.Y. Hwang et al., ''Robot controller with 32-bit DSP chip'' *Proc. Korean Automatic Control Conference* (1991) pp. 292–298.
13. D.H. Cha, ''Shared control of telerobot systems using artificial intelligence algorithms'' *Ph. D. Dissertaion* (Korean Advanced Institute of Science and Technology, 1995).
14. C.A. Desore and M. Vidyasagar, *Feedback Systems: Input–output properties* (Academic Press, New York, 1975).
15. F.L. Lewis, C.T. Abdallah and D.M. Dawson, *Control of Robot Manipulators* (Macmillan Publishing, USA, 1993).
16. M. Uebel, M. Ali and I. Minis, ''The effect of bandwidth on telerobot system performance'' *IEEE Trans. Systems, Man and Cybernetics* **24,** No. 2, 342–348 (1994).
17. D.A. Lawrence, ''Impedance control stability properties in common implementations'' *Proc. IEEE Int. Conf. Robotics and Automation* (1988) pp. 1185–1190.
18. H. Seraji, ''Adaptive admittance control: An approach to explicit force control in compliant motion'' *IEEE Int. Conf. Robotics and Automation* (1994) pp. 2705–2712.
19. D.E. Rumelhart, G.E. Hinton and R.J. Williams, ''Learning internal representations by error propagation'', In: *Parallel Distributed Processing: explorations in the micro structures of cognition* (MIT Press, Cambridge, MA 1986) **Vol. 1,** pp. 318–362.
20. C.C. Lee, ''Fuzzy logic in control systems: Fuzzy logic controller, Part I–II'' *IEEE Trans. Systems, Man and Cybernetics* **20,** No. 2, 404–435 (1990).
21. W.S. Kim, ''Shared compliant control: A stability analysis and experiments'', *Proc. IEEE Int. Conf. Robotics and Automation* (1990) pp. 620–623.
22. W. Books and D.P. Hannema, ''Master-slave manipulator performance for various dynamic characteristics and positioning task parameters'' *J. IEEE Syst., Man, Cybern.* **10,** 764–771 (1980).
23. W.S. Kim, F. Tendick et al., ''A comparison of position and rate control for telemanipulators with consideration of manipulator system dynamics'' *IEEE Trans. Robotics and Automation* **3,** 426–436 (1987).

https://doi.org/10.1017/S0263574797000039 Published online by Cambridge University Press